Overview of Gait Synthesis for the Humanoid COMAN

Chengxu Zhou[1], Xin Wang[12*], Zhibin Li[13], and Nikos Tsagarakis[1]

[1]*Department of Advanced Robotics, Istituto Italiano di Tecnologia, Via Morego 30, 16163 Genova, Italy.*
[2]*Shenzhen Academy of Aerospace Technology, 518057, Shenzhen, China.*
[3]*School of Informatics, University of Edinburgh, 10 Crichton St, Edinburgh EH8 9AB, United Kingdom.*
[*]*Corresponding author, xin.wang@hit.edu.cn*

Abstract

This paper presents the development of a generic gait synthesis for the humanoid robot COMAN. Based on the essential *Gait Pattern Generator*, the proposed synthesis offers enhanced versatilities of bipedal locomotion for different tasks and also provides the data storage and communication mechanisms among different modules. As an outcome, we are able to augment new abilities for COMAN by integrating new control modules and software tools at a cost of a very few modifications. Moreover, the integrated foot placement optimization in the *Gait Pattern Generator* optimizes the referential gait parameters in order to comply with the natural dynamics and kinematics of the robot, which improves the robustness of the implementation on real robots. We have also presented a practical approach to generate pelvis motion from CoM references using a simplified three-point-mass model, as well as a straightforward and effective state estimation using the sensory feedback. Three types of real experiments were studied in an increasing complexity to demonstrate the effectiveness and successful implementation of the proposed gait synthesis on a real humanoid.

Keywords: humanoid robots, bipedal locomotion, gait synthesis, dynamic walking.

1 Introduction

Humanoid robots have been gaining an increasing attention in the recent years due to their improved technological readiness and the potential to have real outdoor applications. With the anthropomorphic morphology, humanoids possess a great potential of completing the tasks undertaken by humans [1]–[3], such as using human-oriented tools, driving vehicles, traversing unstructured terrains where the wheeled robots cannot go, operating in hazardous environment, rescue/repair in disaster responses, and the like. In short, humanoid robots or their variants, as a question of time, earn good motivations under the context of our aging society, and can be deployed as general machines with a fairly large spectrum of skills. The scenarios of exploring
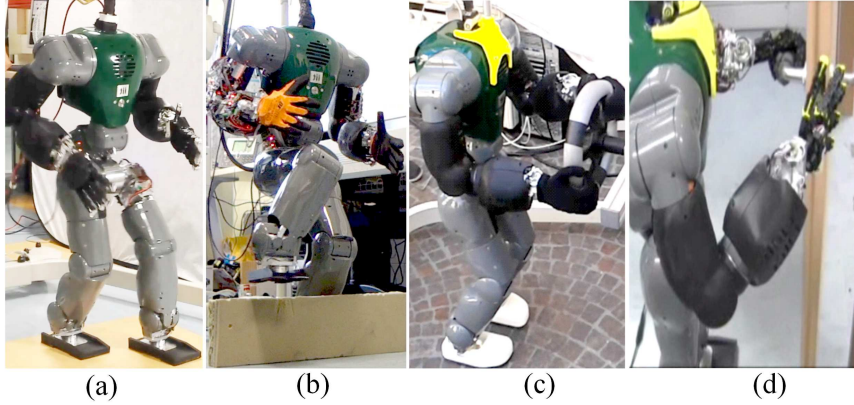
(a)   (b)   (c)   (d)

Figure 1: COMAN's demonstration as a general machine with versatile skills for solving complex tasks in real world scenarios: (a) fast dynamic walking; (b) obstacle negotiation; (c) valve turning; (d) door opening.

humanoid robots as an universal machine are illustrated in Fig. 1 from some research works, such as stepping over a large obstacle [4], that were studied on the COMAN robot [5].

To achieve the completion of tasks in real world, a physical mobility is the fundamental basis. Therefore, a reliable and robust locomotion skill shall be addressed first. Hence, researchers have made tremendous efforts in the past to improve bipedal walking for humanoids. A widely implemented class of gait pattern generations are developed based on the Zero Moment Point (ZMP) [6], such as HUBO [7], ASIMO [8], HRP [9] and the Atlas [10]. The generated gait patterns are then combined with feedback controllers to stabilize the motion of the robot by tracking the planned references at very time instant [11], applying compliance control [12], [13], or reactively replanning the references [14]–[16]. For this class of control, we have a number of options of classical and modern linear controllers to improve the performance and realize different functionalities [17]–[19]. Pratt *et al.* [20] have presented a capturability-based framework for balance and walking control of legged robots. Englsberger *et al.* [21] have successfully implemented the Divergent Component of Motion for realizing the dynamic bipedal gaits. Some other robots, such as MABEL [22] and ATRIAS [23], have adopted a different approach where nonlinear control plays an important role and the finite state machine approach is commonly used. This alternative solution often offers an interesting feature in terms of agility and energy efficiency. However, in turn, its nonlinear feature makes the stability analysis very difficult, and the implementation of 3D walking is rather rare to date.

Research efforts are made on the humanoid robots for improving their adaptivity in human daily environment. This trend is been accelerating after the disaster happened at Fukushima Daiichi nuclear power plant in 2011. The DARPA Robotics Challenge (DRC) was heavily influenced by the events at Fukushima, thus it imposed a big challenge for the locomotion by requiring every robot to operate in outdoor environment without a safety harness. Complex tasks such as stair-climbing, vehicle egress, rough terrain traversal etc. demand advanced locomotion ability. It is critical that every team concentrates in not only developing algorithms

for specific tasks [24], [25], but also integrating different controllers [26]–[29].

During the preparation of the WALK-MAN team for the DRC finals, we were motivated by the tasks requirements, and learned the importance of having a generic locomotion module that can be easily adapted to tasks without too much modifications of an existing framework, which could significantly facilitate system integration. Therefore, in this paper, we present an overview of our gait synthesis which is developed and validated on the COMAN platform that targets on the advanced locomotion skills for humanoid robots. The inherent expendable structure of the proposed synthesis offers enhanced versatilities for the locomotion under different purposes by introducing plug-in modules, and also provides the data storage and communication mechanisms among different modules. As an outcome, we are able to augment new abilities for COMAN by integrating new control modules and software tools at a cost of very few modifications.

The rest of this paper is organized as follows. Section 2 briefly introduces the components of the proposed gait synthesis. Section 3 presents the modules of *Gait Pattern Generator*, such as the optimization of foot placement and step time, the center of mass (CoM) and foot trajectories generation, as well as the three-mass model used for analytically generating the pelvis motion from the CoM/feet trajectories. Section 4 elaborates the main concepts of *Interactive Data Server* and explains two most frequently used services. Section 5 demonstrates the effectiveness of the proposed gait synthesis from three different locomotion tasks. We summarize and conclude our study in Section 6.

2   Overview of the Gait Synthesis

As shown in Fig. 2, the proposed gait synthesis mainly consists of four parts: the essential *Gait Pattern Generator*, *High Level Controller*s, *Walking Plug-in Module*s, *Interactive Data Server* (*IDS*). The COMAN is the testbed for hardware implementation and validation.

The *Gait Pattern Generator* takes the sequence of desired foot placements as inputs and generates reference trajectories to perform dynamic walking. It firstly solves a nonlinear constrained optimization problem to adjust the foothold location and time in order to warrant both kinematic and dynamic feasibilities, then generates ZMP references including gait initiation and termination phases. The horizontal CoM references are therefore produced using a predictive control scheme, combined with the body orientation and vertical CoM motion in the case of non-straight/non-flat walking. The references of CoM will then pass into a simplified dynamics filter in order to obtain the pelvis motion. By solving the inverse kinematics given the pelvis and feet references, the joint angles of lower body are obtained and then sent to the robot. Details of this controller will be explained in Section 3.

The *High Level Controller*s are the modules that provide global settings, environmental information or autonomous decisions that considered as the higher hierarchy in the whole control framework, compared to the *Gait Pattern Generator* and *Walking Plug-in Module*s. For example, user commands, perception, navigation etc. are within this scope, especially the
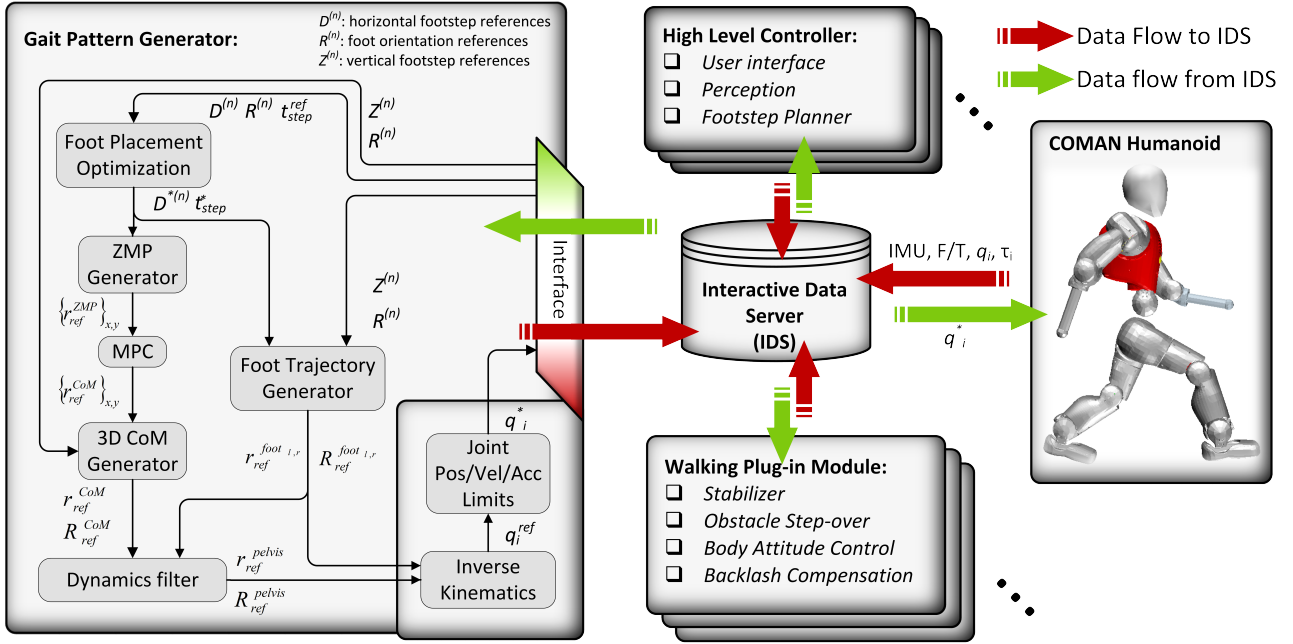
Figure 2: The gait synthesis for the humanoid COMAN.

footstep planner, which generates a sequence of desired foot placements, is a higher level on top of the *Gait Pattern Generator*.

The *Walking Plug-in Module*s play complementary roles in addition to the *Gait Pattern Generator*. They either generate modifications to the references in order to reduce the errors between the desired and real behaviors, such as stabilizer or body attitude controller, or provide additional controllers to the default framework to complete specific tasks, such as obstacle overstepping module.

The *IDS* is an interchange of data and services, all the data, such as parameters, references, sensory feedback etc., related to the above parts are stored, processed in the *IDS* and communicated between different controllers. Moreover, various internal services of the *IDS*, such as sensor fusion, CoM estimation, foot contact detection, coordinates transformation etc., provide further information to the controllers. Details will be explained in Section 4. The COMAN robot as a real platform provides real-time sensory feedback to the gait synthesis and receives joint level commands (joint angle or torque) to perform versatile tasks such as walking, overstepping, door opening etc.

3   Gait Pattern Generation

Gait pattern generation for humanoid robots is challenging, as a feasible motion needs to be chosen from numerous realizable solutions within the robots' kinematics and dynamics. In this section, the framework of *Gait Pattern Generator* is presented. It firstly optimizes the desired footsteps and step time, and then generates trajectories of swing foot and pelvis based on the

optimized footsteps. These references are then sent to inverse kinematics module to obtain joint space references.

3.1 Foot Placement Optimization

Normally, a humanoid is expected to achieve a desired motion state at a desired position. For instance, during DRC tasks, the robot needs to traverse cinder blocks via a sequence of footsteps found by the *High Level Controller*s. However, considering the available workspace defined by the kinematics of the robot, these footsteps do not always need to be strictly constrained to realize the desired motion. Moreover, it shall be noted that these manually appointed gait parameters could conform with the natural dynamics of the robot. Therefore, Foot Placement Optimization module is proposed to make a trade-off between the designed gait and the natural dynamics of the robot.

The humanoid robot can be simplified as a 3D linear inverted pendulum model (LIPM) [30], which consists of the CoM of the robot and a mass-less leg connecting the CoM and the supporting point. The equations of motion of the LIPM are formulated as follows,

$$\boldsymbol{X}_f^{(n)} = \boldsymbol{A}^{(n)} \boldsymbol{X}_i^{(n)} + \boldsymbol{B}^{(n)} \boldsymbol{D}^{(n)}, \tag{1}$$

with

$$\boldsymbol{A}^{(n)} = \begin{bmatrix} C^{(n)} & T_c S^{(n)} & \\ S^{(n)}/T_c & C^{(n)} & \boldsymbol{0}_{2\times 2} \\ & & C^{(n)} & T_c S^{(n)} \\ \boldsymbol{0}_{2\times 2} & & S^{(n)}/T_c & C^{(n)} \end{bmatrix},$$

$$\boldsymbol{B}^{(n)} = \begin{bmatrix} 1 - C^{(n)} & \boldsymbol{0}_{2\times 1} \\ -S^{(n)}/T_c & \\ & 1 - C^{(n)} \\ \boldsymbol{0}_{2\times 1} & -S^{(n)}/T_c \end{bmatrix},$$

where $\boldsymbol{X}_f^{(n)} = [x_f^{(n)}; \dot{x}_f^{(n)}; y_f^{(n)}; \dot{y}_f^{(n)}]$ is the CoM final states in the saggital and lateral planes, $\boldsymbol{X}_i^{(n)} = [x_i^{(n)}; \dot{x}_i^{(n)}; y_i^{(n)}; \dot{y}_i^{(n)}]$ is the CoM initial states at the nth step, $\boldsymbol{D}^{(n)} = [d_x^{(n)}; d_y^{(n)}]$ is the horizontal position of foot placements, $C^{(n)} \equiv \cosh \frac{t_{\text{step}}^{(n)}}{T_c}$, $S^{(n)} \equiv \sinh \frac{t_{\text{step}}^{(n)}}{T_c}$, $t_{\text{step}}^{(n)}$ is the step time at n^{th} step, and $T_c = \sqrt{\frac{z_c}{g}}$ is the time constant of the system, z_c represents the constant CoM height which is 0.448 m for COMAN during walking.

According to (1), the final state of CoM $\boldsymbol{X}_f^{(n)}$ is determined by the references of the foot placements $\boldsymbol{D}^{(n)}$ and the step time $t_{\text{step}}^{(n)}$ as shown in Fig. 3(a). However, these references are usually unnatural for the robot to achieve, and very often have conflicts with the natural dynamics of the point mass model. Therefore, an optimization problem considering the LIPM dynamics is formulated to reach a compromise at each step. The cost function is constructed as

$$\min_{\boldsymbol{U}^{(n)}} \quad \left\| \boldsymbol{Q}(\boldsymbol{X}_f^{(n)} - \boldsymbol{X}_{\text{ref}}^{(n)}) \right\|^2 + \omega \left\| \boldsymbol{D}^{(n)} - \boldsymbol{D}^{*(n-1)} \right\|^2 \tag{2}$$

$$\text{s.t.} \qquad \boldsymbol{D}^{(n)} \in \boldsymbol{S}_r \cap \boldsymbol{S}_a \,,$$

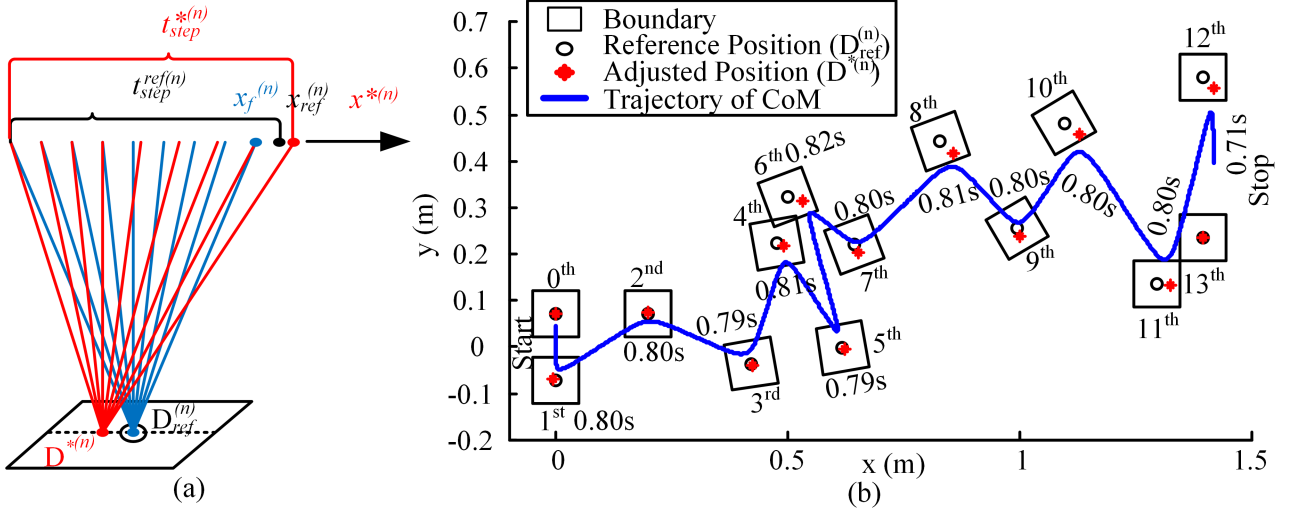$$t_{lb} \leq t_{\text{step}}^{(n)} \leq t_{ub} \,,$$

Figure 3: The concept of foot placement optimization. (a) How the change of COP affects the CoM state in the end of a step. (b) An example of foot placement optimization: black circles are the original foot placement references, red stars are the optimized positions constrained inside the black square boundaries.

while also satisfying the equality constraints (1). $\boldsymbol{U}^{(n)} = [\boldsymbol{D}^{(n)} \; ; \; t_{\text{step}}^{(n)}]$ is defined as the target variables of this optimization problem and $\boldsymbol{U}^{*(n)} = [\boldsymbol{D}^{*(n)} \; ; \; t_{\text{step}}^{*(n)}]$ is the solution at n^{th} step, $\boldsymbol{X}_{\text{ref}}^{(n)}$ is the reference final state of CoM, $\boldsymbol{Q}$ and ω are the weights for different objectives, $\boldsymbol{S}_r$ and $\boldsymbol{S}_a$ represent the rectangular searching area and kinematic reachable area respectively, t_{lb} and t_{ub} are the lower and upper boundaries of the step time.

The optimization formulation (2) is a typical nonlinear constrained quadratic problem. The general method of sequential quadratic programming is used to obtain the local optimal solution $\boldsymbol{U}^{*(n)}$. The first part of the objective function in (2) tries to realize the CoM states approaching the reference states $\boldsymbol{X}_{\text{ref}}^{(n)}$ calculated by the high level defined footsteps reference $\boldsymbol{D}_{\text{ref}}^{(n)}$ and step time reference $t_{\text{ref}}^{(n)}$ using (1). The second part of the objective function tries to minimize the distance between the next footstep and the support foot in order to avoid reaching the limits of the leg's workspace.

Constraints $\boldsymbol{S}_r$ and $\boldsymbol{S}_a$ are updated at each step. As shown in Fig. 4, in order to prevent large deviations from the reference footstep, $\boldsymbol{S}_r$ is set as a 10×10 cm rectangular around $\boldsymbol{D}_{\text{ref}}^{(n)}$ to ensure safe walking without stepping into undesired areas. The reachable kinematic space $\boldsymbol{S}_a$, the area enclosed by the kinematic limit boundary, is calculated considering the joint limits. The kinematic limit, which is similar to the possible landing area in [31], is enclosed by two parts: a straight line at half of hip width away from the stance foot for avoiding crossing legs; the circular curve centered at the stance foot formed by the kinematic limit of the swing leg's workspace. The radius of 0.4 m is used for COMAN in this paper.

As shown in Fig. 3(b), the reference foot placements were designed to perform omni-directional walking, and the reference step time was 0.8 s. The robot firstly walked forward ($0^{th} \sim 2^{nd}$), and turned left with several sidesteps ($3^{rd} \sim 10^{th}$), then turned back ($11^{th} \sim 12^{th}$)
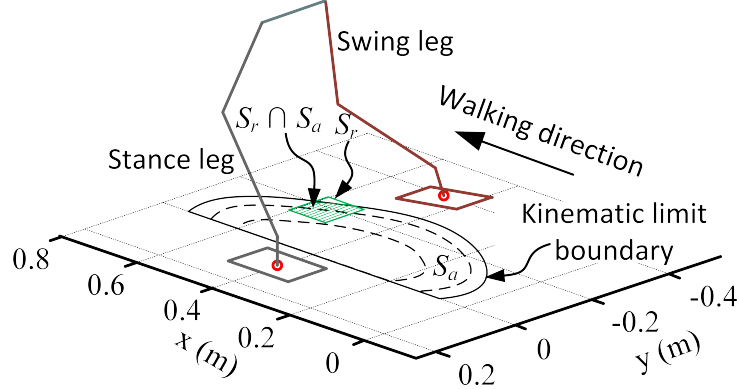
Figure 4: The illustration of nonlinear kinematic constraints in the optimization.

and finally stopped at 13th step. Solving (2), the reference foot placements (black cycles) were adjusted to new locations (red stars), and the duration of each step was optimized as well.

The ZMP references could be generated by consecutively connecting these optimized foot placements. In addition, it is also necessary to design the ZMP references for gait initiation/termination. For further implementation on the robot, 20% of the step time is chosen for the double support phase, which is referenced from human gait analysis [32]. After the ZMP references are generated, a variety of predictive controllers, such as Preview Control [17] or Model Predictive Control [18], can be used to generate horizontal CoM references $\boldsymbol{r}_{\mathrm{ref}}^{\mathrm{CoM}}$. The swing foot trajectory reference $\boldsymbol{r}_{\mathrm{ref}}^{\mathrm{foot}}$ is generated by a template pattern using the target parameters to suit different tasks [4].

3.2 Pelvis Motion Generation

Although, the walking pattern generation method explained so far is horizontal walking centric, the same method can also be used for walking in 3D terrains with small additional control of vertical motion regulation. The CoM motions along z direction and in x-y plane can be decoupled under the assumption of LIPM which restricts the vertical CoM acceleration as zero. The vertical CoM motion can be generated independently by connecting the discrete points which have a constant CoM height with respect to the local footstep. The body rotation $\boldsymbol{R}_{\mathrm{ref}}^{\mathrm{body}}$ is generated by a cubic spline curve continuously changing from step to step. This is similar to the body/leg-simultaneous method in [33]. Herein, the CoM motion is extended to 3D space with the position reference $\boldsymbol{r}_{\mathrm{ref}}^{\mathrm{CoM}}$ and orientation reference $\boldsymbol{R}_{\mathrm{ref}}^{\mathrm{body}}$.

For the inverse kinematics [16], the required inputs are the positions and orientations of the robot pelvis and feet. The reference orientation $\boldsymbol{R}_{\mathrm{ref}}^{\mathrm{body}}$ can be considered the same as the orientation of the pelvis $\boldsymbol{R}_{\mathrm{ref}}^{\mathrm{pelvis}}$, but the CoM position reference $\boldsymbol{r}_{\mathrm{ref}}^{\mathrm{CoM}}$ usually does not coincide with the pelvis position $\boldsymbol{r}_{\mathrm{ref}}^{\mathrm{pelvis}}$ due to the mass distribution of the robot, as shown in Fig. 5. Therefore, the pelvis motions need to resolved from the CoM references.

Similar to [8], the humanoid robot is approximately modeled as three point masses located at the center of upper body m_{ub}, left foot m_{lf} and right foot m_{rf}, respectively. The mass of
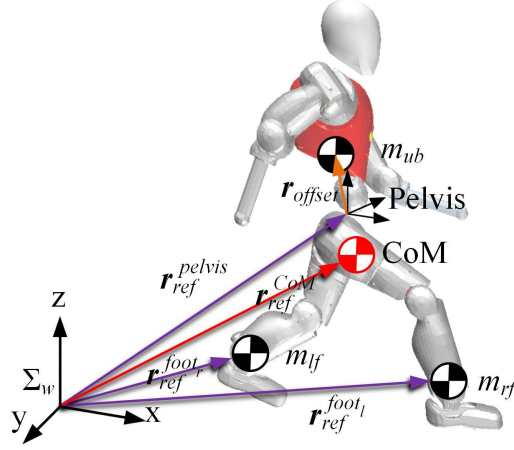
7

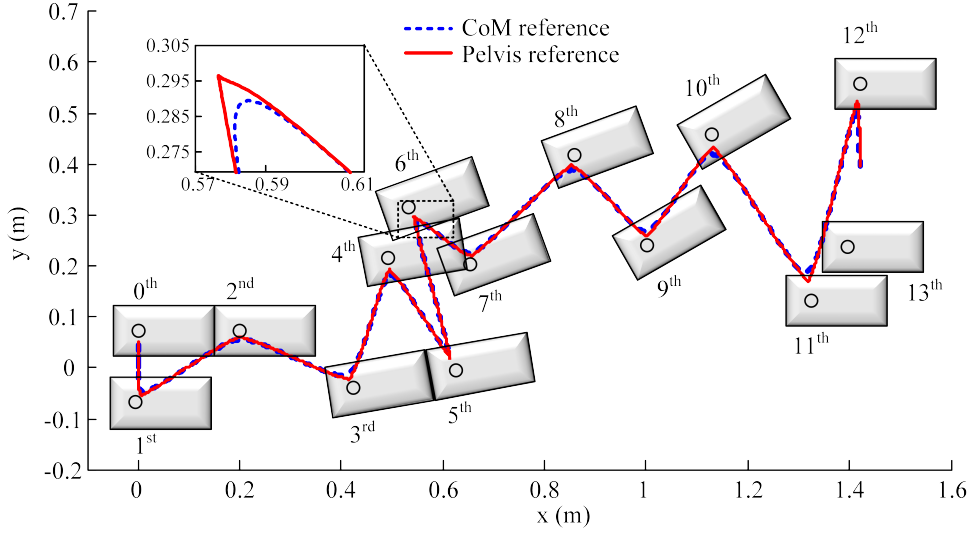Figure 5: Three-mass model used for pelvis motion generation.

Figure 6: The pelvis reference (red solid line) generated by the dynamics filter module using the CoM reference (blue dash line).

one leg is separated into two parts, 77% to m_{ub} and 23% to its foot part mass. Therefore, m_{ub} contains the whole upper body mass and 77% of leg masses, m_{lf} contains the left foot mass and 23% of left leg mass, m_{rf} is the same as m_{lf}. Choosing the world frame Σ_W as the reference frame, the relation between the three point masses model and the CoM is formulated as follows,

$$m_{ub}(\boldsymbol{r}_{\text{ref}}^{\text{pelvis}} + \boldsymbol{R}_{\text{ref}}^{\text{pelvis}}\boldsymbol{r}_{\text{offset}}) + m_{lf}\boldsymbol{r}_{\text{ref}}^{\text{foot}_l} + m_{rf}\boldsymbol{r}_{\text{ref}}^{\text{foot}_r} = m_{\text{tot}}\boldsymbol{r}_{\text{ref}}^{\text{CoM}}, \tag{3}$$

where $\boldsymbol{r}_{\text{offset}}$ is the local offset position vector from pelvis to m_{ub}, $m_{\text{tot}} = m_{ub} + m_{lf} + m_{rf}$ is the total weight of the robot, $\boldsymbol{r}_{\text{ref}}^{\text{foot}_l}$ and $\boldsymbol{r}_{\text{ref}}^{\text{foot}_r}$ are the references of left foot and right foot trajectory, respectively. Therefore, the output of dynamics filter, the pelvis reference $\boldsymbol{r}_{\text{ref}}^{\text{pelvis}}$, could be calculated subsequently.

As shown in Fig. 6, the pelvis motion plotted in red solid line is obtained using (3). Comparing the references of pelvis and CoM, we can see the difference between them due to

8

the distributed masses in feet, as shown in the subplot of Fig. 6. Herein, the inputs of the inverse kinematics module, $r_{\text{ref}}^{\text{pelvis}}$, $R_{\text{ref}}^{\text{pelvis}}$, $r_{\text{ref}}^{\text{foot}_l}$, $R_{\text{ref}}^{\text{foot}_l}$, $r_{\text{ref}}^{\text{foot}_r}$ and $R_{\text{ref}}^{\text{foot}_r}$ in world frame Σ_W, are all obtained for generating joint angles to realize dynamic locomotion tasks.

4 Interactive Data Server

To control walking of a humanoid robot, various data such as sensory feedback, robot states, contact conditions etc., needs to be communicated between controllers. The *IDS* is an interchange of data and services of processed sensory feedback, including a database for storing information and a set of services, which process the raw data and deal with the requests from different controllers.

4.1 Database

The database contains the information communicated between modules. The data can be mainly classified into four categories. The first is the sensory raw data from sensors mounted on the robot such as encoders, torque sensors and IMU etc.. The second is the processed data provided by *IDS* services, such as foot contact conditions and CoM estimations etc.. The third is the intermediate data provided by plug-in modules, such as CoM and ZMP references provided by the gait generator module, the CoM modification from the stabilizer module [12], and the backlash and gravity compensation provided by the compensation module [4] etc.. The last category is the user input parameters such as desired gait parameters, controllers gains, robot dimensions etc..

4.2 Services

There are various types of sensors such as motor encoder, joint torque sensor, ankle force/torque sensor, and inertial measurement unit (IMU) etc., the *IDS* provides services of basic signal conditioning and sensor fusion. Two frequently used services are briefly introduced below.

4.2.1 Foot Contact Condition

The humanoid robot's foot contact conditions are classified as *In Air*, *Right Foot Single Support* (*RFSS*), *Double Support* (*DS*) and *Left Foot Single Support* (*LFSS*), which are determined by the contact status of left and right foot, respectively.

For each foot, if the vertical component of the Ground Reaction Force (GRF), which is sensed by force/torque sensor mounted in the ankle, is greater than a defined threshold continuously for a certain period of time, then this foot is considered to have firm contact with the ground. Vice versa, if the vertical component of the GRF is constantly less than the threshold for a certain period, this foot is considered to have no contact with the ground. The contact condition remains unchanged in other situations. A good trade-off is achieved between the
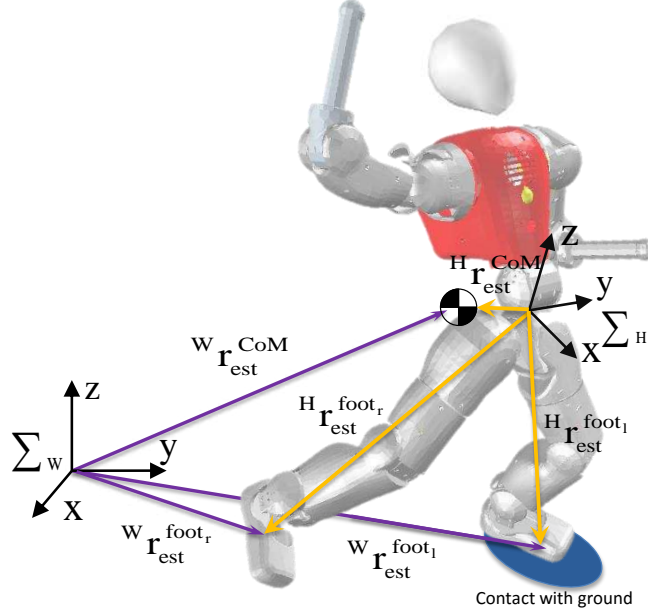
Figure 7: The illustration for CoM estimation service.

delay and signal noise in the decision of foot contact status, we found 20 ms as an appropriate time window for the contact estimation in this study.

4.2.2 Stae Estimation of the CoM

One of the major services is to compute the current CoM state of the robot, namely the position and velocity. Fig. 7 illustrates geometric relation of the robot CoM position in World frame Σ_W. Only joint encoders, IMU and foot force/torque sensors feedback are needed for this service. A local frame located at the center of pelvis link is defined as Σ_H, which is then used as the base frame for updating the position and orientation of all links using the joint encoders readings. Therefore, two rotation matrices ${}^H\boldsymbol{R}_F^l$ and ${}^H\boldsymbol{R}_F^r$ from left and right Foot frames to Hip frame, and two position vectors ${}^H\boldsymbol{r}_{\text{foot}}^l$ and ${}^H\boldsymbol{r}_{\text{foot}}^r$ from the origin of Σ_H to the left and right foot can be updated accordingly. The CoM position in Σ_H is calculated by

$$
{}^H\boldsymbol{r}_{\text{est}}^{\text{CoM}} = \frac{\sum m_i {}^H\boldsymbol{r}_i}{\sum m_i}, \tag{4}
$$

where m_i is the mass of ith link and ${}^H\boldsymbol{r}_i$ is the position vector of ith link's CoM in Σ_H.

Updating the CoM states in the world frame Σ_W is made under an assumption that the support foot is always firmly contacted with the ground without any slippage. Therefore, the CoM position in Σ_W, ${}^W\boldsymbol{r}_{\text{est}}^{\text{CoM}}$, can be simply described as

$$
{}^W\boldsymbol{r}_{\text{est}}^{\text{CoM}} = {}^W\boldsymbol{r}_{\text{est}}^{\text{foot}_{\text{sup}}} + {}^W\boldsymbol{R}_H^{\text{IMU}} \left({}^H\boldsymbol{r}_{\text{est}}^{\text{CoM}} - {}^H\boldsymbol{r}_{\text{est}}^{\text{foot}_{\text{sup}}} \right), \tag{5}
$$

where ${}^W\boldsymbol{R}_H^{\text{IMU}}$ is the rotation matrix from Σ_H to Σ_W which is calculated by the feedback of IMU mounted on the pelvis, $\boldsymbol{r}_{\text{est}}^{\text{foot}_{\text{sup}}}$ denotes the vector pointing to the support foot which is left or right foot depending on the foot contact condition. More accurate CoM state estimation in Σ_W

can be achieved by using the Kalman filter based on the acceleration measurement and visual localization.

However, the support foot is changing discretely during bipedal walking which would introduce discontinuities into CoM estimation, thus deteriorate the quality of calculated CoM. Here, a simple approach is proposed to eliminate this defect by smooth transition between two CoM estimations from both feet, the resulted $^W\boldsymbol{r}^{\text{CoM}}_{\text{est}}$ utilizes the weight of vertical GRF of each foot as

$$^W\boldsymbol{r}^{\text{CoM}}_{\text{est}} = \frac{f^l_z \, ^W\boldsymbol{r}^{\text{CoM}_l}_{\text{est}} + f^r_z \, ^W\boldsymbol{r}^{\text{CoM}_r}_{\text{est}}}{f^l_z + f^r_z}, \tag{6}$$

where $^W\boldsymbol{r}^{\text{CoM}_l}_{\text{est}}$ and $^W\boldsymbol{r}^{\text{CoM}_r}_{\text{est}}$ are the CoM in Σ_W calculated by (5) using left and right leg kinematic chain, respectively, f^l_z and f^r_z are the vertical GRF sensed by force/torque sensors mounted on the each foot.

The second assumption is that the foot contact condition has no *In Air* phase during walking, meaning that the foot contact condition only changes between single and double support cyclically. This assumption presumes the robot would not bounce off the ground during foot landing impact. Therefore, the continuity of the vertical GRF guarantees continuous update of the CoM estimate.

The global position of each foot in Σ_W is updated only during its swing phase by

$$\begin{cases} ^W\boldsymbol{r}^{\text{foot}_l}_{\text{est}} &= ^W\boldsymbol{r}^{\text{foot}_r}_{\text{est}} + ^W\boldsymbol{R}^{\text{IMU}}_H(^H\boldsymbol{r}^{\text{foot}_l}_{\text{est}} - ^H\boldsymbol{r}^{\text{foot}_r}_{\text{est}}), & RFSS \\ ^W\boldsymbol{r}^{\text{foot}_r}_{\text{est}} &= ^W\boldsymbol{r}^{\text{foot}_l}_{\text{est}} + ^W\boldsymbol{R}^{\text{IMU}}_H(^H\boldsymbol{r}^{\text{foot}_r}_{\text{est}} - ^H\boldsymbol{r}^{\text{foot}_l}_{\text{est}}), & LFSS \end{cases} \tag{7}$$

using the service presented in Section 4.2.1. The origin of Σ_W is defined as the geometry center of the support polygon when the foot contact condition is in double support DS in the very beginning, the initial positions of each foot, $^W\boldsymbol{r}^{\text{foot}_l}_{\text{est}}$ and $^W\boldsymbol{r}^{\text{foot}_r}_{\text{est}}$, are calculated afterwards.

5 Experiments

This section presents three experiments of locomotion tasks carried out on COMAN in an increasing complexity order. The first experiment validated the proposed *Gait Pattern Generator* could generate feasible references for dynamic walking. However, due to the discrepancies between the theoretical model and the imperfect real world, the *Gait Pattern Generator* needs additional *Walking Plug-in Modules* such as a stabilizer [12] to bridge the gap of between the ideal model and the real system. Their synthesis demonstrates the effectiveness while COMAN performing omni-directional walking in the second experiment. The last experiment is a decent example to demonstrate the work flow of the gait synthesis in completing an obstacle negotiation task.

5.1 Straight Walking

In the first experiment, three straight walking tests were performed with the gait parameters as follows: step time 0.9 s, lift height 0.05 m, double support ration 20% and step length from
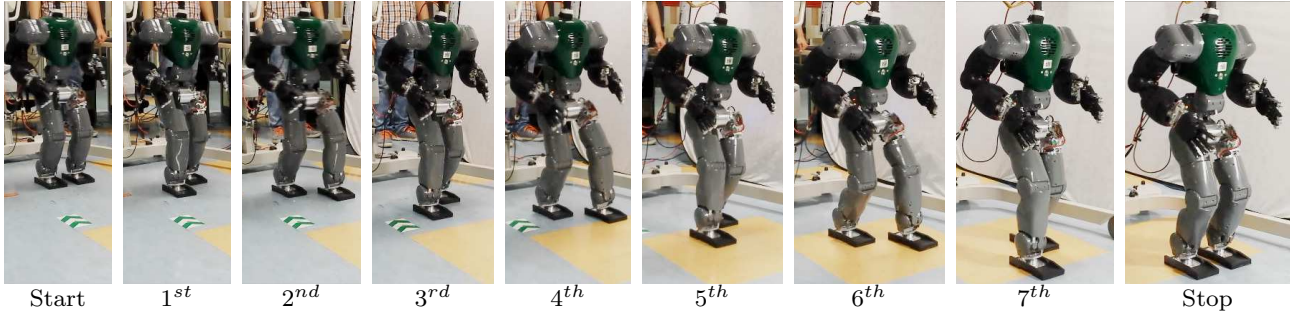
Figure 8: Snapshots of walking forward with step length 0.2 m and stabilizer module on.

0.1 m, 0.15 m to 0.2 m respectively. Each test was repeated by 5 trials.

Table 1: Success rate of the straight walking experiment.

Plug-in Module	Step Length			Total
	0.1 m	0.15 m	0.2m	
None	5/5	4/5	0/5	9/15
Stabilizer	5/5	5/5	5/5	15/15

Table 1 shows the success rate of these three tests. The successful tests were the ones where the COMAN robot completed the whole gait in a stable manner by taking at least 7 steps. It can be found that the first two tests were performed well with only the references generated by the *Gait Pattern Generator* without the stabilizer. However, when the step length increased to 0.2 m, COMAN fell down due to the tracking deterioration caused by the discrepancies between the simplified model and the real robot, e.g. foot-ground impacts in particular. Therefore, one of the *Walking Plug-in Module*s, the stabilizer [12], was activated for long step length walking. The 100% success rate shows that, the plug-in did well as the complementary role that helped the robot to eliminate the disturbances coming from the environmental and modeling errors. Fig. 8 shows one successful trail of COMAN robot walking forward with step length of 0.2 m.

The feasibility of the proposed gait synthesis was validated through simple gait in the previous experiment, further tests were conducted in the following experiments in more complicated scenarios.

5.2 Omni-directional Walking

The omni-directional walking was carried out as the second validation scenario in order to demonstrate the proposed gait synthesis's performance in more general walking case. The gait started with double support on the ground, and the feet during walking were designed to be level to the ground. The nominal step time was 0.9 s, and the foot lift height was 0.04 m. The robot performed totally 14 steps, the step length changed alternately between 0.1 m and 0.05 m from step to step, and the step width was 0.05 m. The robot kept turning 5 degrees per step to the left during the first 7 steps, and then 5 degrees per step to the right during the last
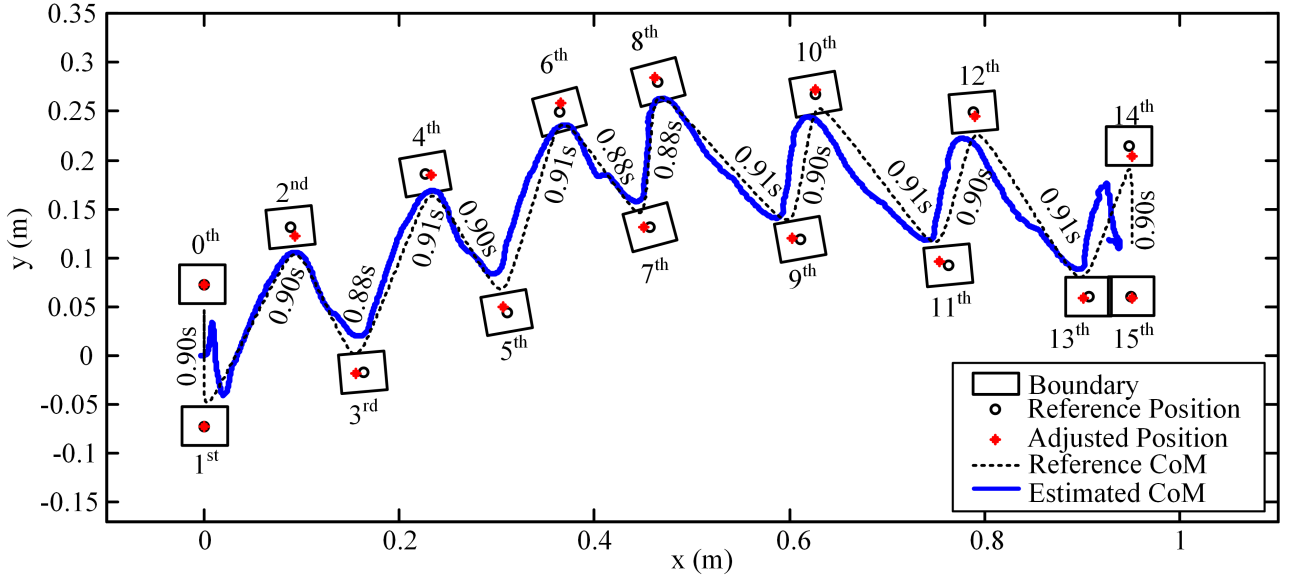
Figure 9: The results of the omni-directional walking experiment. Black circles denote the foot placement references, red stars denote the optimized foot placements with the black square boundaries. The CoM reference (black dash line) is generated by the optimized foot placements. The blue solid line is the real CoM trajectory estimated by the *IDS* service.

7 steps. Therefore, the gait used for this experiment combined walking forward, side stepping and turning, which covered most walking primitives on flat ground.

The COMAN robot successfully completed the full gait pattern with the plug-in stabilizer activated. Fig. 9 shows the foot placement references by black circles, and the optimized ones by red stars. The CoM reference generated based on optimized foot placements is depicted in black dashed line and the estimated COM trajectory is shown by the blue solid line. The difference between the two was partly because of the limited accuracy of the CoM estimation from *IDS*, and also partly because the foot indeed slipped slightly from step to step. Therefore, as number of steps increased, the drift between the ideal and real spatial trajectories of the CoM became unavoidable.

5.3   Stepping Over A Large Obstacle

The last experiment was dedicated to a specific capability of humanoids: stepping over a large obstacle. The obstacle was a block with dimensions of 0.1 m height by 0.05 m width. The collision check module inside the plug-in module [4] decides the gait to walk over the obstacle with the step length of 0.24 m, the lift height of 0.12 m, and the step time of 1.5 s (20% double support phase), and considers the foot size (0.14×0.09 m) of COMAN and its kinematic limits, as well as the 0.01 m safe margin around the obstacle. The *Gait Pattern Generator* therefore generates the joint angle references using the desired footsteps together with the additional modifications provided by the plug-in modules, such as pelvis rotation, hip abduction, backlash and gravity compensation [4].

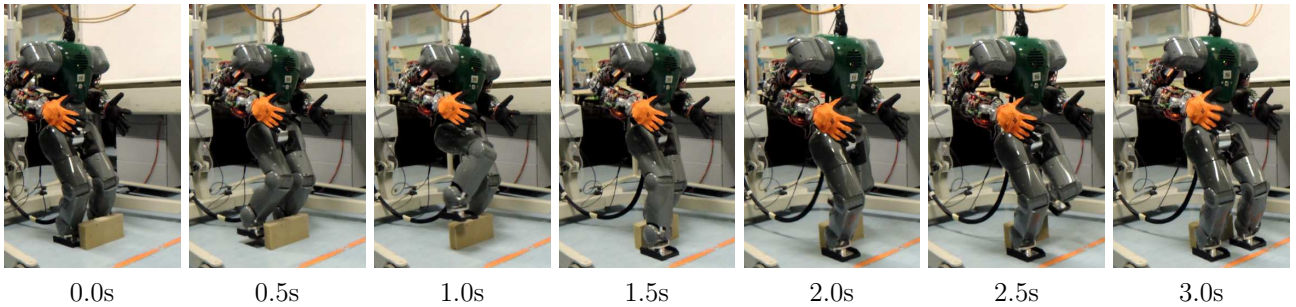| 0.0s | 0.5s | 1.0s | 1.5s | 2.0s | 2.5s | 3.0s |

Figure 10: Snapshots of successful stepping over a large obstacle.

Thanks to the proposed gait synthesis, COMAN was capable of stepping over the obstacle which was almost 20% of its leg length. Fig. 10 shows the front view of COMAN whilst stepping over this large obstacle.

6   Conclusion

In this paper, we present the overview and validation of the proposed gait control synthesis developed for the humanoid COMAN. It aims at enhancing locomotion skill of humanoids by integrating a *Gait Pattern Generator*, *High Level Controller*s, *Walking Plug-in Module*s and a centered *Interactive Data Server*. By implementing the proposed gait synthesis on COMAN, successful demonstrations of various locomotion tasks were performed in an increasing complexity. The first straight walking experiment shown that the basic locomotion capability of the proposed gait synthesis was realized on the humanoid COMAN, and by simply activating the stabilizer, the locomotion quality was significantly improved. The effectiveness of the integration was then further validated by an omni-directional waking experiment. The performance of both the foot placements optimization and the state estimation were successfully demonstrated as well. The capability of overstepping large obstacle using the same gait synthesis was also proved by the physical experiment.

For the future work, on the one hand, different *Walking Plug-in Module*s could be developed to improve the humanoid robots' adaptability in walking or other specific locomotion tasks, such as reactive stepping, dancing, balancing using whole body contacts etc.. On the other hand, introducing state-in-art technologies into *High Level Controller*s for improving the robot's perceptual ability and better autonomy could also be an interesting research direction to make humanoid robots as reliable human companions.

Acknowledgment

References

[1] M.-H. Chiang and F.-R. Chang, "Anthropomorphic design of the human-like walking robot," *Journal of Bionic Engineering*, vol. 10, no. 2, pp. 186–193, 2013.

[2] T. Li, M. Ceccarelli, M. Luo, M. A. Laribi, and S. Zeghloul, "An experimental analysis of overcoming obstacle in human walking," *Journal of Bionic Engineering*, vol. 11, no. 4, pp. 497–505, 2014.

[3] H. Zhu, M. Luo, T. Mei, J. Zhao, T. Li, and F. Guo, "Energy-efficient bio-inspired gait planning and control for biped robot based on human locomotion analysis," *Journal of Bionic Engineering*, vol. 13, no. 2, pp. 271–282, 2016.

[4] C. Zhou, X. Wang, Z. Li, D. Caldwell, and N. Tsagarakis, "Exploiting the Redundancy for Humanoid Robots to Dynamically Step Over a Large Obstacle," in *IEEE/RSJ International Conference on Intelligent Robots and Systems*, Hamburg, Germany, Sep. 2015, pp. 1599–1604.

[5] N. Tsagarakis, S. Morfey, G. Medrano-Cerda, Z. Li, and D. Caldwell, "Compliant humanoid coman: optimal joint stiffness tuning for modal frequency control," in *IEEE International Conference on Robotics and Automation*, 2013, pp. 665–670.

[6] M. Vukobratovic and B. Borovac, "Zero-moment point - thirty five years of its life," *International Journal of Humanoid Robotics*, vol. 1, pp. 157–173, 2004.

[7] J. Kim, I. Park, and J. Oh, "Walking control algorithm of biped humanoid robot on uneven and inclined floor," *Journal of Intelligent & Robotic Systems*, vol. 48, no. 4, pp. 457–484, 2007.

[8] T. Takenaka, T. Matsumoto, and T. Yoshiike, "Real time motion generation and control for biped robot-1st report: walking gait pattern generation," in *IEEE/RSJ International Conference on Intelligent Robots and Systems*, Oct. 2009, pp. 1084–1091.

[9] S. Kajita, M. Morisawa, K. Harada, K. Kaneko, F. Kanehiro, K. Fujiwara, and H. Hirukawa, "Biped Walking Pattern Generator allowing Auxiliary ZMP Control," *IEEE/RSJ International Conference on Intelligent Robots and Systems*, vol. 2, pp. 2993–2999, Oct. 2006.

[10] R. Tedrake, S. Kuindersma, R. Deits, and K. Miura, "A closed-form solution for real-time zmp gait generation and feedback stabilization," in *IEEE-RAS 15th International Conference on Humanoid Robots*, 2015, pp. 936–940.

[11] S. Kajita, M. Morisawa, K. Miura, S. Nakaoka, K. Harada, K. Kaneko, F. Kanehiro, and K. Yokoi, "Biped walking stabilization based on linear inverted pendulum tracking," in *IEEE/RSJ International Conference on Intelligent Robots and Systems*, 2010, pp. 4489–4496.

[12] C. Zhou, Z. Li, X. Wang, N. Tsagarakis, and D. Caldwell, "Stabilization of Bipedal Walking Based on Compliance Control," *Autonomous Robots*, vol. 40, pp. 1041–1057, Aug. 2016.

[13] Z. Li, N. Tsagarakis, and D. Caldwell, "Stabilizing humanoids on slopes using terrain inclination estimation," in *IEEE/RSJ International Conference on Intelligent Robots and Systems*, 2013, pp. 4124–4129.

[14] J. Urata, K. Nshiwaki, Y. Nakanishi, K. Okada, S. Kagami, and M. Inaba, "Online decision of foot placement using singular LQ preview regulation," in *IEEE-RAS International Conference on Humanoid Robots*, 2011, pp. 13–18.

[15] J. Castano, Z. Li, C. Zhou, N. Tsagarakis, and D. Caldwell, "Reactive Gait Generation for Humanoid Robots Based on Analytic Foot Placement Control," *International Journal of Humanoid Robotics*, vol. 13, 1550041 (44 pages), 2016.

[16] C. Zhou, C. Fang, X. Wang, Z. Li, and N. Tsagarakis, "A Generic Optimization-based Framework for Reactive Collision Avoidance in Bipedal Locomotion," in *IEEE Conference on Automation Science and Engineering*, Fort Worth, TX, USA, Aug. 2016.

[17] S. Kajita, F. Kanehiro, K. Kaneko, K. Fujiwara, K. Harada, K. Yokoi, and H. Hirukawa, "Biped walking pattern generation by using preview control of zero-moment point," in *IEEE International Conference on Robotics and Automation*, vol. 2, 2003, pp. 1620–1626.

[18] P.-B. Wieber, "Trajectory free linear model predictive control for stable walking in the presence of strong perturbations," in *IEEE-RAS International Conference on Humanoid Robots*, Dec. 2006, pp. 137–142.

[19] Y. Tassa, T. Erez, and W. D. Smart, "Receding horizon differential dynamic programming," in *Advances in neural information processing systems*, 2008, pp. 1465–1472.

[20] J. Pratt, T. Koolen, T. De Boer, J. Rebula, S. Cotton, J. Carff, M. Johnson, and P. Neuhaus, "Capturability-based analysis and control of legged locomotion, Part 2: Application to M2V2, a lower-body humanoid," *The International Journal of Robotics Research*, vol. 31, no. 10, pp. 1117–1133, 2012.

[21] J. Englsberger, C. Ott, and A. Albu-Schäffer, "Three-dimensional bipedal walking control based on divergent component of motion," *IEEE Transactions on Robotics*, vol. 31, no. 2, pp. 355–368, 2015.

[22] H.-W. Park, A. Ramezani, and J. Grizzle, "A finite-state machine for accommodating unexpected large ground-height variations in bipedal robot walking," *IEEE Transactions on Robotics*, vol. 29, no. 2, pp. 331–345, 2013.

[23] S. Rezazadeh and J. W. Hurst, "Toward step-by-step synthesis of stable gaits for underactuated compliant legged robots," in *IEEE International Conference on Robotics and Automation*, Seattle, WA, USA, 26-30 May, 2015, pp. 4532–4538.

[24] M. Morisawa, N. Kita, S. Nakaoka, K. Kaneko, S. Kajita, and F. Kanehiro, "Biped locomotion control for uneven terrain with narrow support region," in *IEEE/SICE International Symposium on System Integration (SII)*, Dec. 2014, pp. 34–39.

[25] J. Luo, Y. Zhang, K. K. Hauser, H. A. Park, M. Paldhe, C. S. G. Lee, M. Grey, M. Stilman, J.-H. Oh, J. Lee, I. Kim, and P. Y. Oh, "Robust ladder-climbing with a humanoid robot with application to the darpa robotics challenge," in *IEEE International Conference on Robotics and Automation*, Hong Kong, China, May 2014, pp. 2792–2798.

[26] M. Johnson, B. Shrewsbury, S. Bertrand, T. Wu, D. Duran, M. Floyd, P. Abeles, D. Stephen, N. Mertins, A. Lesman, J. Carff, W. Rifenburgh, P. Kaveti, W. Straatman, J. Smith, M. Griffioen, B. Layton, T. de Boer, T. Koolen, P. D. Neuhaus, and J. E. Pratt, "Team ihmc's lessons learned from the DARPA robotics challenge trials," *Journal of Field Robotics*, vol. 32, no. 2, pp. 192–208, 2015.

[27] S. Feng, E. Whitman, X. Xinjilefu, and C. G. Atkeson, "Optimization-based full body control for the darpa robotics challenge," *Journal of Field Robotics*, vol. 32, no. 2, pp. 293–312, 2015.

[28] S. Kuindersma, R. Deits, M. Fallon, A. Valenzuela, H. Dai, F. Permenter, T. Koolen, P. Marion, and R. Tedrake, "Optimization-based locomotion planning, estimation, and control design for the atlas humanoid robot," *Autonomous Robots*, pp. 1–27, 2015.

[29] M. Zucker, S. Joo, M. X. Grey, C. Rasmussen, E. Huang, M. Stilman, and A. Bobick, "A general-purpose system for teleoperation of the DRC-HUBO humanoid robot," *Journal of Field Robotics*, vol. 32, no. 3, pp. 336–351, 2015.

[30] S. Kajita, H. Hirukawa, K. Harada, and K. Yokoi, *Introduction to Humanoid Robotics*, ser. Springer Tracts in Advanced Robotics. Springer, 2014, vol. 101.

[31] K. Nishiwaki and S. Kagami, "Strategies for adjusting the zmp reference trajectory for maintaining balance in humanoid walking," in *IEEE International Conference on Robotics and Automation*, 2010, pp. 4230–4236.

[32] M. W. Whittle, *Gait analysis: an introduction*. Butterworth-Heinemann, 2014.

[33] J.-C. Lu, J.-Y. Chen, and P.-C. Lin, "Turning in a bipedal robot," *Journal of Bionic Engineering*, vol. 10, no. 3, pp. 292–304, 2013.